Michael Cox (1941–1989): His Pioneering Contributions to Ocean Circulation Modeling

KIRK BRYAN

GFDL/NOAA, Princeton, New Jersey

(Manuscript received 10 September 1990, in final form 17 December 1990)

ABSTRACT

Michael Cox was a pioneer in the development and application of numerical models to the study of the ocean circulation. His simulation of the response of the Indian Ocean to the monsoons was one of the first applications of a numerical model to seasonal changes in circulation near the equator. Cox's finding that the seasonal reversal of the Somali Current was primarily due to local monsoon-driven coastal upwelling challenged a popular theory that the effects of remote forcing, propagating westward along the equatorial waveguide, were the most important mechanism. In a detailed follow-up study, he was able to demonstrate that remote forcing could only be important near the equator along the Somali Coast and that local driving was the only viable mechanism to explain the amplitude and phase of the main features of the seasonal reversal of the Somali Current.

In another pioneering calculation, Cox was the first to simulate the seasonal changes of the eastern equatorial Pacific, including the Legeckis waves between the South Equatorial Current and the Equatorial Counter Current. From his analysis, he concluded that the Legeckis waves were due to both baroclinic and barotropic instability.

Using observed temperature and salinity data, Cox carried out a new type of diagnostic study of the circulation of the World Ocean. His calculations demonstrated the great importance of adjusting the observed density field in a manner compatible with the constraints imposed by the conservation of mass, temperature, and salinity.

In a detailed comparison of simulations of ocean circulation in eddy- and noneddy-resolving models of simplified geometry, Cox was able to demonstrate that mesoscale eddies could have some very important effects on midlatitude thermocline ventilation by wind-driven downwelling. In particular, the mixing by mesoscale eddies along isopycnal surfaces could be strong enough to erase tracer and potential vorticity gradients over trajectories of less than 2000 km. On the other hand, Cox found that poleward transport of buoyancy was approximately the same in similar runs, which did, or did not, include mesoscale eddies. He concluded that this was due to eddy-time mean flow compensation. A similar phenomenon exists in the weakly driven flows of the earth's stratosphere.

1. Introduction

To many, Cox is known for developing and documenting an ocean circulation model and widely sharing it with modelers all over the world. In part due to his natural modesty, his scientific achievements over two decades have been somewhat overshadowed by his widely appreciated efforts in scientific cooperation. The pioneering studies, which he carried out with so much creativity and attention to detail, have done a great deal toward establishing numerical modeling as a recognized approach to studying the ocean.

In 1962 Cox chose to work at the U.S. Weather Bureau's General Circulation Laboratory (now NOAA's Geophysical Fluid Dynamics Laboratory) because it was most consistent with his technical interests and his beliefs as a religious conscientious objector. His first job was operating the IBM "Stretch" computer, a behemoth computer of the day but less powerful than many of today's desktops. He quickly rose to positions of greater responsibility. In 1973–74 Cox attended the University of Washington as a graduate student in oceanography, an experience he valued greatly.

It is obviously impossible to include all his papers in this review, and the choice of only four studies carried out in the 1970s and 1980s was somewhat arbitrary. Cox received NOAA's Environmental Research Laboratories Distinguished Author Award three times, twice for papers that he coauthored and once for a paper for which he was the sole author. In this review, the focus is on papers he wrote as a lead author. In the early part of his research career, his interest was primarily in equatorial oceanography. He prepared the ground for much of the numerical modeling activity connected with tropical air–sea interaction of the last decade. In recent years his attention turned to higher latitudes and the problems of mesoscale eddies and water mass formation. Conspicuously lacking in this review is a discussion of his last paper "An idealized model of the World Ocean. Part I: The global scale water masses" (Cox 1989). This paper was intended to provide some insight on the fundamental processes that determine the water-mass distribution of the

Corresponding author address: Dr. Kirk Bryan, GFDL/NOAA, Princeton University, P.O. Box 308, Princeton, NJ 08540.

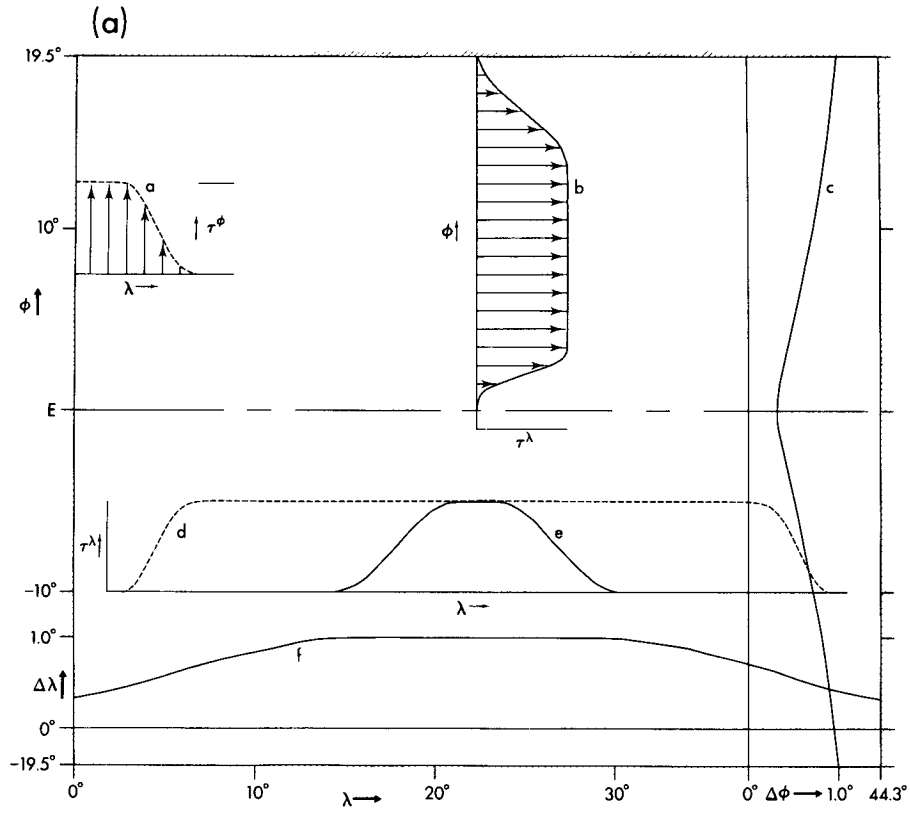
(a)
19.5°
10°
E
-10°
1.0°
0°
-19.5°
0°
10°
20°
30°
0° Δφ → 1.0° 44.3°
λ →
φ ↑
Δλ ↑
τ^φ ↑
τ^λ ↑
a
b
c
d
e
f

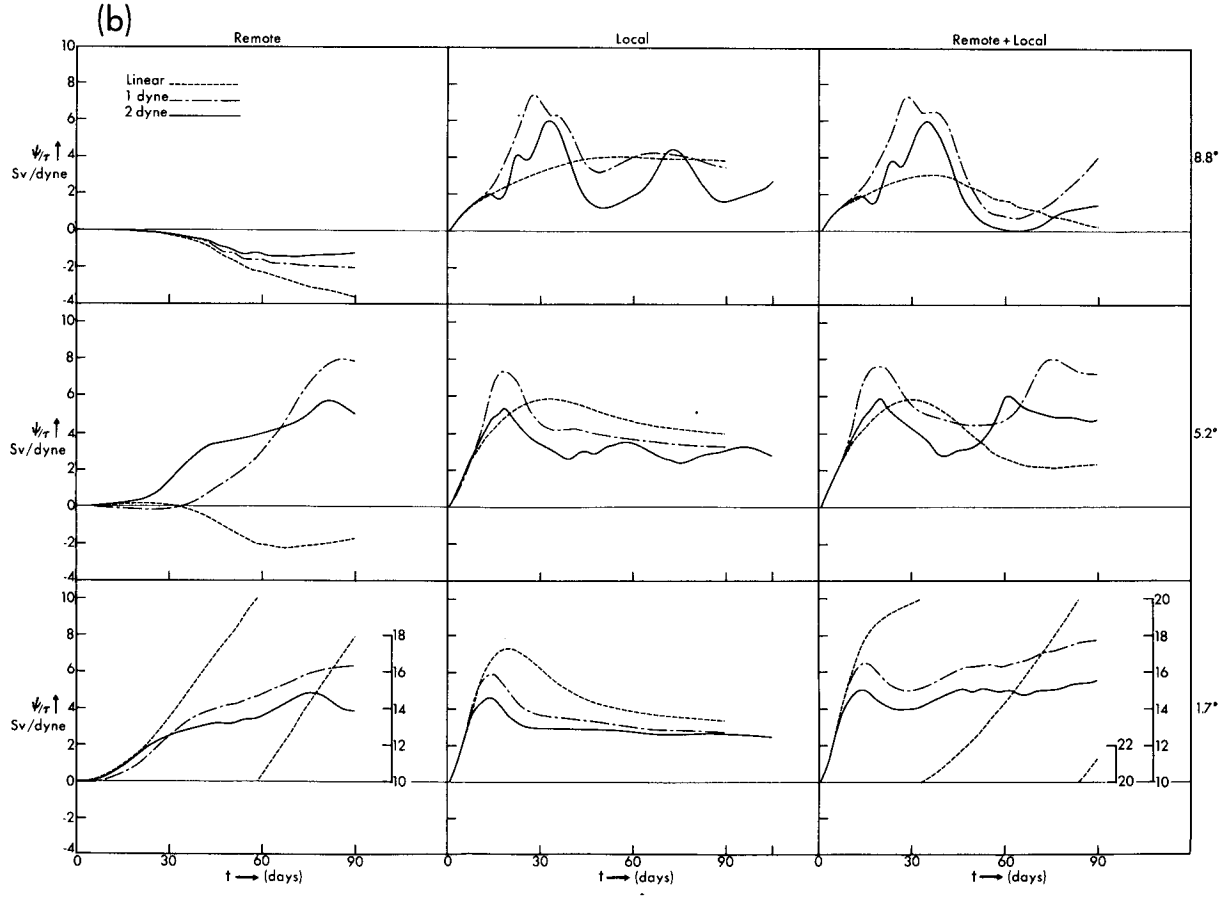
(b)
Remote
Local
Remote + Local
Linear
1 dyne
2 dyne
ψ/τ ↑ Sv/dyne
8.8°
5.2°
1.7°
t → (days)
0
30
60
90

oceans. The approach will probably inspire many follow-up efforts. This paper was only published less than a year ago, however, and it is probably too early to determine its full significance.

2. Cox's (1970) study of the response of the Indian Ocean circulation to the monsoon

In looking at surface drift maps for the World Ocean, the clearest signature of seasonal change is the reversal of the Somali Current in the western Indian Ocean. Cox's study of Indian Ocean circulation was motivated by the observations of the Indian Ocean Expedition and the desire to test the new ocean model being developed at the General Circulation Laboratory (now GFDL) of the U.S. Weather Bureau. Up to that point almost all modeling studies had been carried out for idealized geometries, which do not allow meaningful comparison with observations.

Cox's (1970) original study involved a calculation for the entire Indian Ocean on a six-level, $4° \times 4°$ latitude–longitude grid. The initial integration extended over 130 years. The grid was refined to a $2° \times 2°$ grid and carried out for another 55 years. In the final stage, an additional layer was included, and the grid was refined to a $1° \times 1°$ grid. This final stage was only integrated for 7 years. The entire calculation was a real tour de force when one considers that it was carried out on a primitive supercomputer of the 1960s with a speed of less than one million instructions per second and a core memory of less than one-third of a megabyte. Most desktop computers today have greater memory and speed.

The final high-resolution stage of the calculation contained a simulation of the reversal of the currents with season along the Somali coast, which was quite realistic in terms of width and vertical penetration in comparison with direct current measurements of Swallow and Bruce (1966). The model was not able to capture the extremely high amplitude of the summer jet, which often exceeds 3 m s^{-1}, but the timing of the onset of the northward flowing current appeared to be accurately simulated. Based on this result, Cox (1970) described the coastal jet as a response to the upwelling caused by the onset of the summer monsoons blowing in a northward direction parallel to the coast.

A very different viewpoint was put forward in a study that appeared just a few months before Cox's paper was published. Unaware of the earlier studies by Blandford (1966) and Matsuno (1966), Lighthill (1969) independently derived the dispersion relations for the trapped equatorial modes. Lighthill proposed that the Somali ocean jet was primarily the response to remote winds over the interior. The signal would then be carried along the equatorial waveguide to the western boundary. Lighthill's elegant theory received widespread attention and gave a new impetus to the study of equatorial dynamics.

In a follow-up study, Cox (1976) constructed an idealized model of the Indian Ocean, which included the simulation of equatorially trapped waves. He then carried out careful tests to determine whether the three-dimensional numerical model gave the correct dispersion of equatorially trapped waves compared to analytical results. After obtaining good agreement, he carried out a series of carefully designed numerical experiments. The forcing fields are shown in Fig. 1a, and the response for the Somali Current is shown in Fig. 1b. It is obvious that the time scale of the response to remote forcing shown in Fig. 1b is of the order of one month, while the response to local forcing is of the order of days. A Somali current simulated by remote winds grows at a much slower rate than observed and separates from the coast much closer to the equator than observed. As can be seen in Fig. 1b, the remote winds actually force a southward current at 8.8°N, while the observed current is to the north. Cox (1976) concluded that local forcing dominates the early growth phase of the Somali summer current and is essential for its extension northward along the Somali coast.

3. Numerical modeling of the equatorial Pacific

Infrared images from geostationary satellites over the Pacific (Legeckis 1977) indicate a train of remarkably regular troichoidal waves is moving westward between the equator and the Equatorial Countercurrent to the north. The signature of these waves is in the temperature contrast between the relatively cold equatorial waters and the much warmer waters at higher latitudes. The annual appearance of these waves is closely associated with the waxing and waning of the Equatorial Countercurrent. The waves only appear when wind conditions are favorable for strong upwelling at the equator and a strong countercurrent. The waves have a wavelength of about 1000 km and the north–south displacement of isotherms associated with them is several hundred kilometers. Unlike most large-scale waves in atmospheric flow, the waves propagate westward with little tendency to amplify and break. Philander (1978) predicted that the source of energy for the waves arose from shearing instability between the South Equatorial Current and the Equatorial Countercurrent.

It was suggested (Philander 1978) that waves generated by instabilities in the near-surface currents could be propagated downward in the equatorial waveguide,

FIG. 1. (a) Wind-stress forcing fields used by Cox (1976) in his study of local and remote response of the Somali Current. Curves a, b, d, and e indicate the distribution of local and remote windforcing. Curves c and f show the finite difference gridpoint spacing with greater resolution near the boundaries. (b) The response of the Somali Current in the model as a transport normalized by the stress amplitude. Units are 10^9 kg (dyn s)$^{-1}$. The latitude of the response is shown to the right of the panels.

providing an energy sink that could account for the unusual tendency of the "Legeckis waves" not to amplify as they propagated westward.

This phenomenon motivated a seminal study of the seasonal regime of the equatorial Pacific (Cox 1980), which paved the way for high-resolution tropical ocean models that have since been extensively explored by others (for a recent review, Philander 1989). The Pacific between 30°N and 30°S is included in the model. Temperature and salinity were damped to their observed values close to the open boundaries using a small time constant. Long-term drift of interior water-mass properties below 1000 m was prevented by damping to observations using a 6-month time constant. Observed temperatures and salinities are forced at the surface of the model using a 1-month time constant. The Wyrtki and Meyers (1976) wind-stress dataset was also specified at the upper boundary. Meridional resolution was 0.5° of latitude, and the zonal resolution 1° of longitude with 14 levels in the vertical. The geometry and the summer sea surface temperature pattern are indicated in Fig. 2.

The simulation was very successful in imitating the seasonal onset of the Legeckis waves at the correct time of year and location. To analyze the waves in more detail, the instability of the zonal currents of the basin scale was studied within a smaller channel model with cyclic boundary conditions. Based on this analysis, Cox (1980) was able to conclude that a significant source of energy for the waves came from lateral shear between the South Equatorial Current and the Equatorial Countercurrent in agreement with Philander's (1978) earlier analytic study. However, baroclinic instability was also a contributor, indicating a mixed type of instability. Radiation of energy away from the generating region in the model appeared to take place through the agency of three types of waves. One type was external Rossby waves, which are extremely effective in radiating energy in a meridional direction. Another type was Rossby–gravity waves with a large eastward group velocity and small vertical energy propagation. The third type was internal Rossby waves, which were the most effective in transferring energy downward into the deep ocean in the vicinity of the equator.

4. Cox's (1975) model of the World Ocean

A very significant conference was sponsored by the U.S. National Academy of Sciences in October 1972. The proceedings were published in "Numerical Models of Ocean Circulation" (NAS 1975). At that time Cox presented a calculation that illustrates some of the basic issues in reconstructing the ocean circulation from the density observations. For many oceanographers, a diagnosis of the ocean circulation from observations was synonymous with the classical problem of finding a geostrophic reference velocity. In other words, it was felt that density measurements were adequate to calculate the baroclinic component of the velocity field, and the only requirement for determining the ocean circulation was a determination of the barotropic component from the equations of motion and continuity (Sarkisyan and Ivanov 1971; Holland and Hirschman 1972). Through a systematic series of experiments, Cox (1975) showed the importance of including the constraints imposed by the temperature and salinity equations as well. This same approach was incorporated a few years later in inverse models (Schott and Stommel

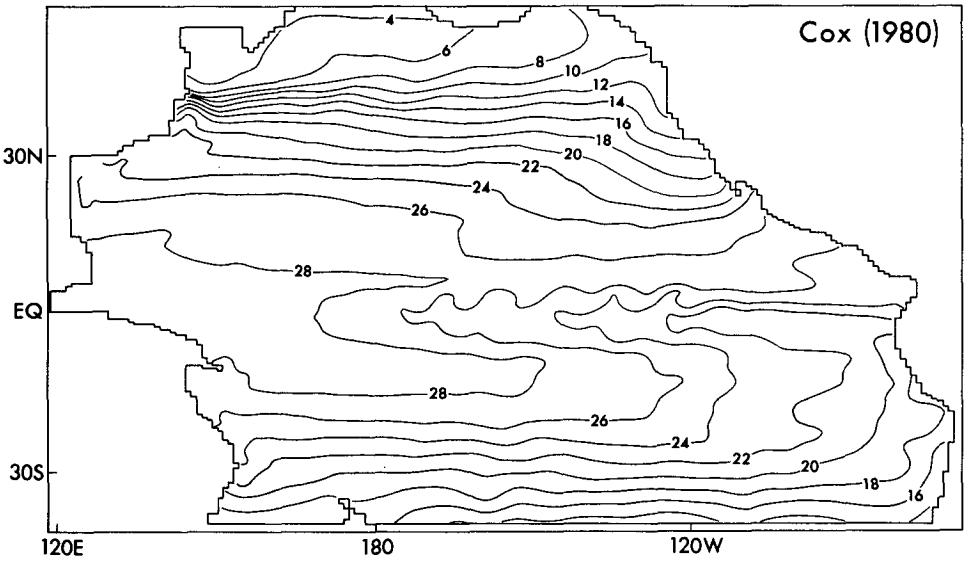

FIG. 2. The geometry of Cox's (1980) model of the equatorial Pacific Ocean used to study 30-day waves. The sea surface temperature is shown for the summer period. Note the Legeckis waves adjacent to the equator in the eastern Pacific.

1978; Wunsch 1978). As in the case of Cox's Indian Ocean numerical experiment, the entire calculation was carried out on the Univac 1108 computer, which had the capability of computing at a little over one million instructions per second. Cox (1975) compared the results of three numerical experiments. The calculations using the Bryan (1969) model made use of a 2° × 2° grid extending from 62°N to 62°S, supplemented by two polar grids on different projections of the same resolution. The grids were joined by interpolation. Experiment I was the case of homogeneous density already considered by Bryan and Cox (1972). The flow in this case is purely driven by wind and is highly constrained by the bottom topography of the ocean. Primary features are weak anticyclonic gyres in the subtropical zones of the North Atlantic and Pacific. In the Southern Hemisphere large amplitude gyres are present in the southern Indian and south Atlantic oceans. Topography prevents the transport through the Drake Passage from exceeding 20×10^9 kg s^{-1}. The results confirm the work of Munk and Palmen (1951) that the Munk wind-driven model with or without bottom topography fails to give even a first-order description of the actual Southern Ocean circulation.

Experiment II includes a fixed, nonhomogeneous density field specified from observations and corresponds to the earlier diagnostic studies noted above. The baroclinic effect introduced in this way clearly releases the circulation from the strong topographic constraint indicated in Experiment I. This is clearest in the Southern Ocean sector. The transport through the Drake Passage is almost ten times larger than in the homogeneous case in Experiment I. The Circumpolar Current is no longer deflected by the submarine ridge of the eastern South Pacific. Experiment III represented the final results of a 2.3-year numerical integration using the NODC hydrographic data as initial conditions on temperature and salinity. The adjustment of the temperature and salinity fields in the relatively short 2.3-year calculation results in a much smoother mass transport pattern compared to either Experiment I or Experiment II. The large subtropical wind gyres of the Northern Hemisphere are much closer to the patterns one would infer from the observed dynamic topography. The same is true for the subtropical gyres of the Southern Hemisphere. The total transport through the Drake Passage remains about the same level as in Experiment II, which is about 200×10^9 kg s^{-1}. This is about 50% higher than recent measurements indicate (Whitworth and Peterson 1985).

Recently Semtner and Chervin (1988) carried out a calculation for the World Ocean using a mesh size of 1/2° by 1/2° of latitude and longitude. Unlike Cox's (1975) experiment III, temperature and salinity were damped to the observed value with a damping time of a month at the surface and years at subsurface levels. This method is similar to the "robust diagnostic" model of Sarmiento and Bryan (1982). Figure 3 allows a comparison of the streamfunction patterns for the Semtner and Chervin (1988) model and Cox's experiment III for the South Atlantic and Drake Passage region. In spite of the differences in resolution and mixing, the total transport predicted in the Circumpolar Current is about 200×10^9 kg s^{-1} in both cases. In the Southern Ocean the patterns of flow are quite similar.

A controversy exists over the contribution of the Indonesian flow through to the thermohaline circulation of the World Ocean. Estimates (Piola and Gordon 1984; Toole et al. 1988) vary from 0 to 10×10^9 kg s^{-1}. A comparison of Cox's (1975) analysis of the meridional circulation of the South Pacific with inverse calculations of Wunsch et al. (1983) shown in Table 1 provide some insight on the large-scale implications of the flowthrough. In the Wunsch et al. (1983) inverse calculations, the flowthrough is assumed to be zero, while the Cox model found the flowthrough to be very large (18×10^9 kg s^{-1}). A similar value was found in general circulation calculations carried out by Semtner and Chervin (1988). In both cases the predicted transport value may be somewhat of an artifact of the simplified geometry of the Indonesian region assumed in the models.

In spite of this very different flowthrough transport, it is surprising how much transport estimates given in Table 1 have in common for bottom and deep waters. As we examine Table 1, we see that both studies predict inflows of bottom water of 8–12 ($\times 10^9$ kg s^{-1}) from the Southern to the Pacific oceans. Both studies also indicate a comparable transport of deep waters from the Pacific Ocean back out into the Southern Ocean. The implication is that the net amount of bottom and deep water incorporated in the upper waters of the Pacific is only the small difference between these large flows as pointed out by Fiadeiro (1982), who obtained a similar estimate of about 12×10^9 kg s^{-1} for the recycling of deep and bottom water.

This circulation scheme is quite different from a simple conveyor belt concept in which bottom water flows into the Pacific and exists as surface water through the Indonesian flowthrough. However, it should be pointed out that the net effect on the global heat balance is nearly the same.

The significant differences between the model transports and the inverse transports exist in the upper kilometer of the water column. Table 1 suggests that the model adjustment to the flowthrough transport is entirely in the upper ocean and that the deep geostrophic transports are determined geostrophically from the initial temperature and salinity data. Thus, the density data requires the same deep overturning in both the general circulation model and the inverse calculations, but relatively rapid geostrophic adjustment in the upper water column in the model allows it to accommodate itself to a flow around the Australian continent of nearly 20×10^9 kg s^{-1}. This mode of adjustment is particu-

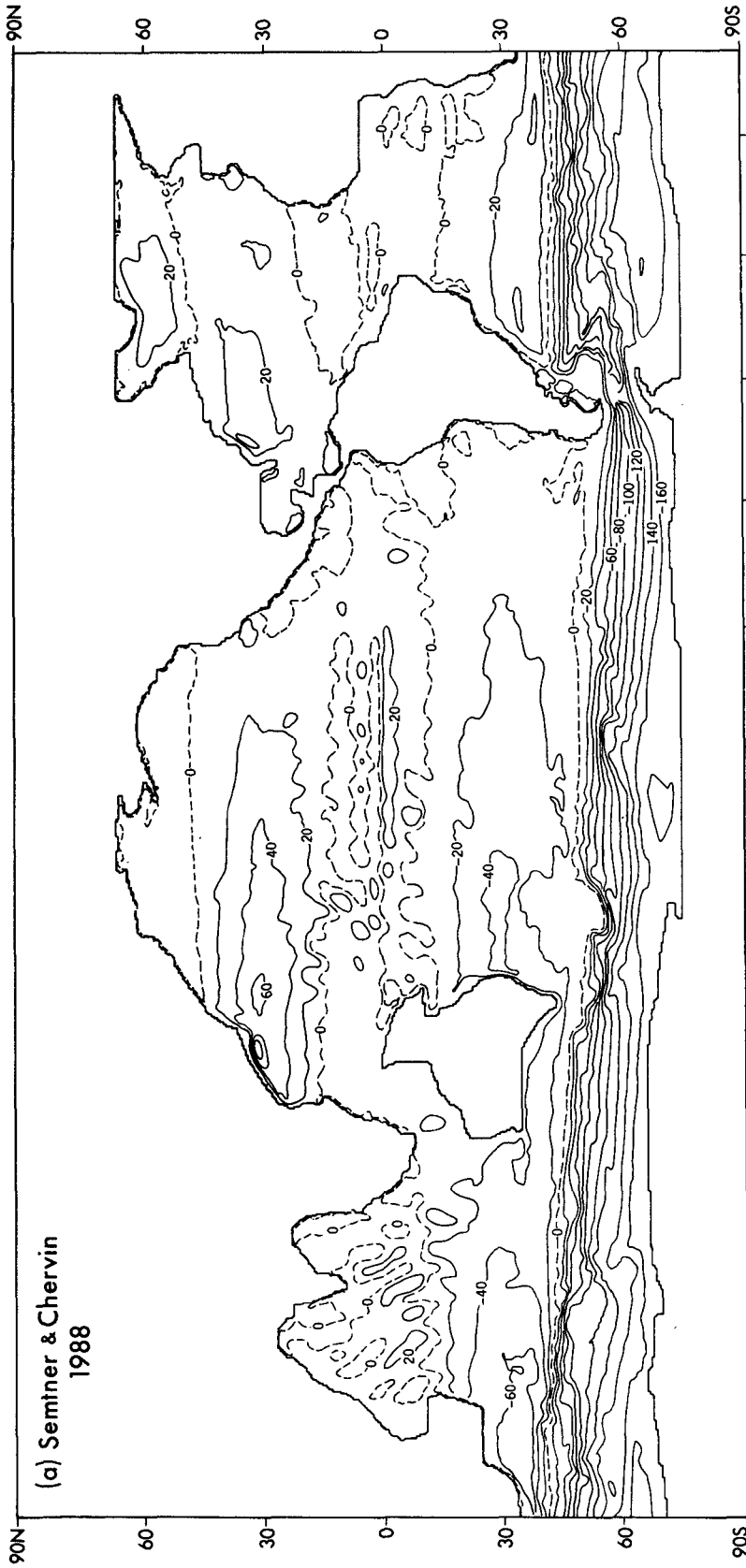

FIG. 3. The transport streamfunction in a model of the World Ocean. (a) Semtner and Chervin's (1988) high-resolution model in latitude–longitude coordinates. (b) Cox's (1975) experiment III in mercator coordinates.

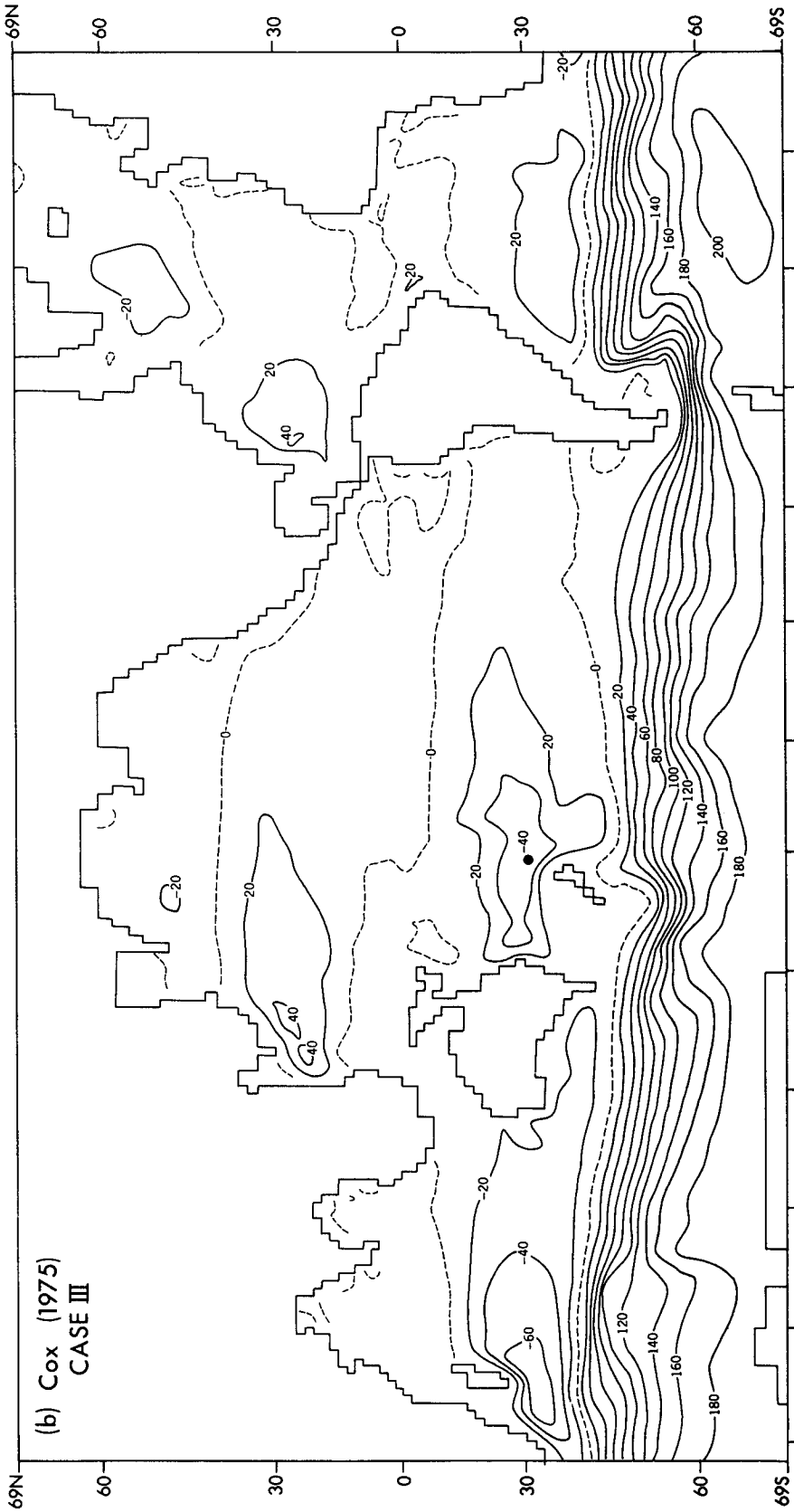

FIG. 3. (*Continued*)

TABLE 1. Transports for given depth intervals zonally integrated across the entire South Pacific from experiment III of Cox (1975, Fig. 7) and from the inverse calculation of Wunsch et al. (1983) from the Scorpio data. Positive sign indicates northward transport.

Depth interval (km)	Cox (1975) (10^9 kg s^{-1})	Wunsch et al. (1983) (10^9 kg s^{-1})
	28°S Pacific	
0.0–0.45	10.0	−1.6
0.45–1.22	5.4	1.2
1.22–2.30	−3.0	−7.3
2.30–3.07	−3.0	−5.3
3.07–3.49	0.0	0.6
3.49–	8.6	12.4
Sum	18.0	0.0
	43°S Pacific	
0.0–0.49	16.0	1.0
0.49–1.21	6.0	0.5
1.21–2.37	−8.0	−10.2
2.37–3.08	−4.0	−3.0
3.08–3.57	0.0	1.6
3.57–	8.0	10.2
Sum	18.0	0.1

larly interesting in view of the large changes in sea level in the western equatorial Pacific, which are known to be associated with different phases of El Niño. It seems reasonable that the Indonesian flowthrough would be modulated by these pressure variations. Cox's model suggests that temporal variations in the flowthrough could be easily accommodated by a change in the surface-water flow around Australia.

It is clear that Cox's (1975) experiment III represents a pioneering contribution to combining a model and hydrographic data, which will serve as a guide to future efforts in inverse modeling as WOCE (World Ocean Circulation Experiment) datasets become available.

5. A hierarchy of models of the ventilated thermocline

Cox put a great deal of effort into creating a very general model that could be applied to realistic simulations of ocean circulation. However, he also believed that the greatest insights could be gained from numerical experiments carried out in a more idealized geometry. Testing ideas was his primary motivation. Without the complications of irregular bottom topography, Cox felt it was easier to use numerical experiments to form a link between analytic theories and the real ocean. During the 1980s he launched a series of studies, which have proven to be particularly successful in achieving that goal.

The transient tracers released by the bomb tests of the late 1950s and early 1960s have provided dramatic evidence (Sarmiento et al. 1982) that important downward pathways existed to the deep waters of the ocean other than in the high polar areas of the World Ocean. Tongues of tritium moving along density surfaces of the subtropical gyre of the North Atlantic served to emphasize the importance of intermediate water formation, which had been somewhat overlooked with more emphasis being placed on deep- and bottom-water formation at higher latitudes. The widespread use of quasi-geostrophic models for analyzing ocean dynamics made it difficult to handle intermediate water formation, since a quasi-geostrophic model could not include direct pathways from a surface outcrop to the base of the thermocline.

A more general analytic framework for this process was proposed by Luyten et al. (1983), which was called the "ventilated thermocline" model. A visit by Joseph Pedlosky, one of the authors of this model, to Princeton in 1982 inspired Cox and Bryan (1984) to set up an experiment to gain a better understanding of the relation of the "ventilated thermocline" model to the rest of the ocean circulation. Many aspects of the analytic theory are highly idealized. For example, an ideal fluid flow is assumed without friction or diffusion. Simplified assumptions must be made about side-wall boundary conditions. On the other hand, it was not clear that a numerical model could be constructed that would even approximate the ideal fluid equation in the interior of the basin. Thus, the motivation was to provide a test of both the analytic theory and the capability of the numerical model.

The model consists of a sector between two meridians 60° of longitude apart, extending from the equator to 65°N. The model has a uniform depth of 4 km. Realistic values of wind stress and density are specified at the surface as a function of latitude only. Vertical diffusion has a uniform value of 0.3 cm^2 s^{-1}, and the horizontal resolution was approximately 1° by 1° in latitude and longitude. One of the important contributions of the Luyten et al. (1983) paper and earlier studies was to define three regions in the lower thermocline with distinctly different flow regimes. One was the "pool" region, which has closed trajectories on an isopycnal surface. As noted by Ierley and Young (1983), a segment of these closed trajectories coincides with the western boundary current. The "shadow" region lies along the eastern equatorial flank of the subtropical gyre. This is an unventilated region that cannot be reached directly from trajectories originating at outcrops. The third region is the "ventilated" region in which trajectories form vertical pathways directly from the surface to the base of the thermocline along isopycnal surfaces.

The model was integrated to an equilibrium state using some of the acceleration methods outlined by Bryan (1984). Lateral viscosity and diffusion are great enough to suppress lateral and vertical shear instability. Trajectories along an isopycnal surface are shown in Fig. 4a. The distribution of potential vorticity is also shown in the same figure. For an "ideal" fluid, thermocline potential vorticity would be uniform along the trajectories. The fact that the trajectories cut across

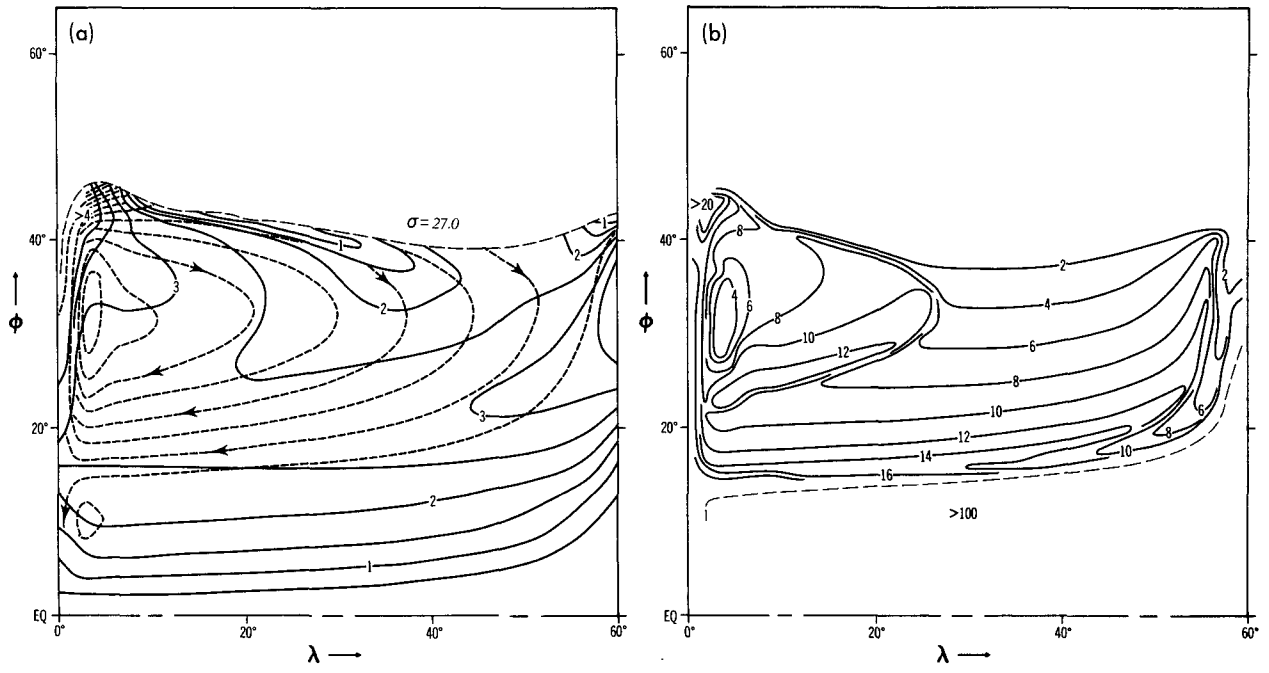

FIG. 4. Results from Cox and Bryan (1984). (a) Geostrophic streamlines and potential vorticity on the sigma = 27.0 surface. (b) Advective time since exposure to the surface calculated for the sigma = 27.0 surface.

lines of constant potential vorticity clearly shows that dissipative effects are important. Figure 4b shows a map of the time elapsed along the trajectory since contact with the surface is in years. The values range from 2 years close to the outcrop on the polar side of the gyre to 16 years along the equatorial flank of the gyre. On the equatorial flank of the gyre, the time constant increases abruptly to over 100 years, corresponding to the "shadow" region not directly accessible from the surface. To the west there is a steep age gradient bounding a "pool" region of closed trajectories. Within the pool region, ages of only 4 years near the western boundary indicate mixing with the surface. In addition, the solution clearly contains another region not included in the "ventilated thermocline" theory. This region noted by Colin de Verdiere (1988) arises from the viscous and diffusive eastern boundary layer. The boundary layer permits high potential vorticity water to form along the wall and leak out along density surfaces.

With the exception of the viscous and diffusive "leak" region at the eastern boundary, the model reproduces the main features of the ventilated thermocline theory in spite of the existence of dissipative effects. Further insight is provided on the relation of convection to potential vorticity distributions by the analysis shown in Fig. 5. The upper panel shows a plan view of a steady-state trajectory, which originates in the center of the subtropical gyre, then traces through the western boundary current into a convective region in the eastward drift between the subtropical and subarctic gyres. The trajectory starts at only 29 m below the surface at −15.4 years. It takes over 5 years for the trajectory to spiral downward to 172 m as it enters the western boundary current at 20°N.

The particle moves rapidly northward in the western boundary current, climbing 30 m. Only 0.2 years is required to move over 2000 km to the point of separation of the western boundary current. At this point the particle speed is again reduced, and 2 years are required to traverse a similar distance through the convective region. In the convective region the particle descends, regaining the depth lost in the western boundary current. Reentering the subtropical gyre, the particle speed slows further and descent continues. Over a period of 7 years the trajectory moves downward at approximately one meter per month, compared to a rate twice that in the first 5 years of the trajectory from −15.4 to −9.9 years.

The change of absolute potential vorticity along the trajectory is shown in Fig. 5b. The potential vorticity is quite uniform along the first part of the trajectory, which is in the interior of the basin. In the western boundary current the potential vorticity increases. Some of this increase may be offset if the effects of relative vorticity were included, since the relative vorticity on the interior flank of the western boundary current is anticyclonic. An increase of anticyclonic relative vorticity along the western boundary current would tend to balance the increase in coriolis parameter as the fluid is displaced poleward. As the trajectory turns eastward at 40°N into the convective zone, the

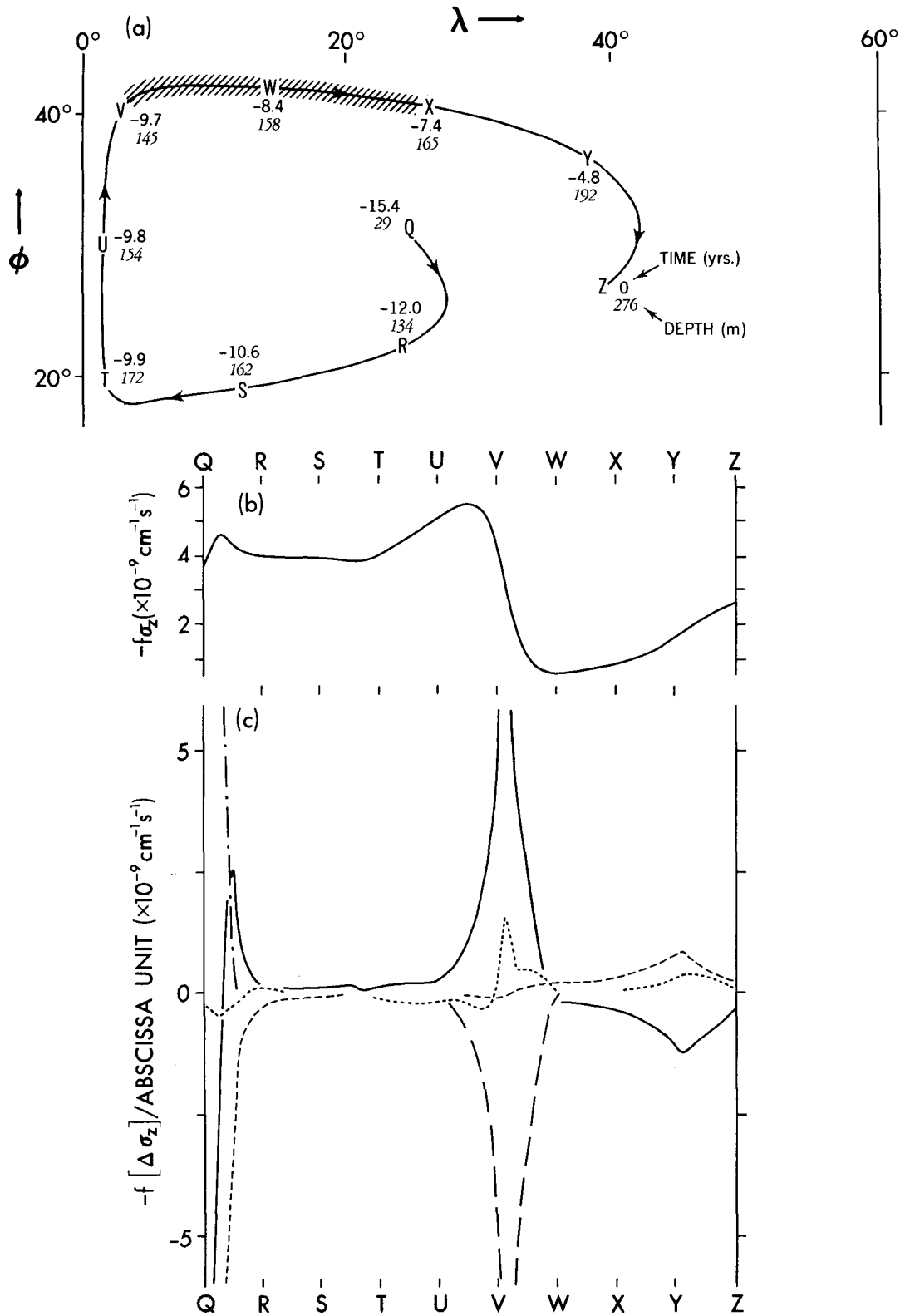

FIG. 5. (a) A particle trajectory corresponding to the steady state solution of Cox and Bryan (1984). (b) The change of absolute potential vorticity along the trajectory. (c) The coriolis force times the change of stratification along the trajectory. The terms are convection (long dashes), advection (solid lines), horizontal mixing (dots), vertical mixing (short dashes).

potential vorticity abruptly decreases. The balance of terms that change stratification along the trajectory are shown in Fig. 5c. At point "V" in the convective zone, the convective term has a large negative component, which is balanced by advection. This means that the convection destroys stratification, but lateral advection balances this process by bringing in new water with greater stratification from the south. On the final leg of the trajectory (W–Z), the sign of the advection term reverses. Advection is introducing poorly stratified waters into the main subtropical thermocline through the ventilation process. In an ideal fluid model of the thermocline, potential vorticity would be exactly conserved along this leg of the trajectory. In Fig. 5c we see that vertical diffusion always tends to increase the stratification.

The analysis shown in Fig. 5 describes the process of change in potential vorticity along only one of many possible trajectories. However, it gives a flavor of the effects of convection and diffusion in the destruction and creation of stratification in the subtropical gyre. The Cox and Bryan (1984) study provided a link between numerical models of low resolution and the Luyten et al. (1983) "ventilated" thermocline model, but left open the question of the effect of mesoscale eddies. To include mesoscale eddies Cox (1985, 1987) extended the model to much higher resolution, increasing the number of horizontal grid points by a factor of three in each direction. The fine grid model was initialized from a near equilibrium solution on the course grid and run an additional 24 years. This is not enough time to allow the ocean model to come to equilibrium, but as Cox demonstrated by showing the surface eddy kinetic patterns, it does permit a reasonable adjustment of the upper 500 m.

One of the most interesting results to come out of Cox's (1985) high-resolution model concerns the observed lack of strong gradients of potential vorticity on isopycnal surfaces at the base of the thermocline in subtropical gyres. Rhines and Young (1982) suggested that the primary cause for the observed uniformity of potential vorticity was the existence of closed velocity trajectories on isopycnal surfaces. According to this idea, closed trajectories would isolate "pool" regions of the thermocline, and even a very small amount of lateral mixing would produce homogenization of potential vorticity. As noted previously, however, Ierley and Young (1983) demonstrated in numerical experiments that one segment of "pool" trajectories had to pass through the western boundary current where "strong" mixing would be present. Luyten et al. (1983) commented on this controversy and suggested that the observations of nearly uniform vorticity could be explained in terms of ventilation. Their suggestion was simply that the ventilated waters entering the lower thermocline would have a rather low, nearly uniform potential vorticity to begin with. Thus no mixing would be required to form a nearly uniform potential vorticity pattern on isopycnal surfaces at the base of the thermocline.

Cox (1985) found that mixing by mesoscale eddies was sufficiently vigorous that gradients could be mixed out in only a partial circuit of the subtropical gyre. This led Cox (1985) to conclude that lateral mixing could be important as Rhines and Young (1982) had suggested, but on a much faster time scale. This view appears to be supported by the modeling and analysis of tritium data in the North Atlantic (Sarmiento 1983).

Perhaps the most interesting conclusion from this study concerns the role of mesoscale eddies in poleward buoyancy transport. In this simplified model, temperature and salinity were not considered separately, so that buoyancy transport is a surrogate for heat transport. Bryan (1987) has shown that the heat transport in a simplified geometry model is very sensitive to the level of vertical mixing. It might also be anticipated that the existence or nonexistence of a vigorous mesoscale eddy field would have a strong influence on the poleward transfer of buoyancy. Surprisingly, Cox's (1985) eddy-resolving model showed that was not the case. The buoyancy-driven, meridional overturning is modified by the eddy field in such a way that a near compensation takes place, resulting in no net change in poleward buoyancy transport relative to the non–eddy-resolving case.

Cox's conclusions concerning mesoscale eddies and poleward buoyancy transport are buttressed by calculations with a similar model carried out recently (see Böning 1991). In a model of the same geometry, but including low random bottom topography. Böning increased the resolution to $1/6°$ by $1/6°$ latitude and longitude. This allows a much better representation of mesoscale eddies.

6. Discussion

Phillips (1956) coined the term "numerical experiment" for his numerical simulations of the atmosphere's general circulation. The term is a good one, but all too often the expected standards of planning and interpretation in other experimental fields have been lacking in studies involving numerical experimentation. By example, Michael Cox did a great deal to raise the level in numerical experimentation for the study of the ocean circulation.

In oceanographic research an unfortunate gap tends to exist between modeling and theory on the one hand and measurement and analysis on the other. To bridge this gap there is a strong incentive for modelers to attempt to simulate observations as closely as possible in their numerical experiments. While this is a laudable tendency, Michael Cox was always concerned about the difficulties of interpreting numerical experiments for complex geometry and realistic, but complex, boundary conditions. His principal goal was in the testing of ideas and in designing the least encumbered framework for doing so. Obviously the requirements

of climate and data assimilation will require a broad spectrum of modeling activities in the years ahead. However, an important lesson of Michael Cox's research is that in the long run, the power of computer models combined with the judicious application of "Bishop Occam's razor" will provide an important tool for progress.

Acknowledgments. The author thanks James Luyten, J. R. Toggweiler, and George Philander for providing ideas for this review.

REFERENCES

Blandford, R., 1966: Mixed Rossby–gravity waves in the ocean. *Deep-Sea Res.*, **13**, 941–961.

Böning, C., 1991: Eddies in a primitive-equation model: Sensitivity to horizontal resolution. *J. Phys. Oceanogr.*, **21**,

Bryan, F. O., 1987: Parameter sensitivity of primitive equation ocean circulation models. *J. Phys. Oceanogr.*, **17**, 970–985.

Bryan, K., 1969: A numerical method for the study of the circulation of the World Ocean. *J. Comput. Phys.*, **4**, 347–376.

——, 1984: Accelerating the convergence to equilibrium of ocean climate models. *J. Phys. Oceanogr.*, **14**, 666–673.

——, 1986: Poleward buoyancy transport in the ocean and mesoscale eddies. *J. Phys. Oceanogr.*, **16**, 927–933.

——, and M. D. Cox, 1972: The circulation of the World Ocean. Part I: A homogeneous model. *J. Phys. Oceanogr.*, **2**, 319–335.

Colin de Verdiere, A., 1988: Buoyancy-driven planetary flows. *J. Mar. Res.*, **46**, 215–265.

——, 1989: On the interaction of wind and buoyancy driven flows. *J. Mar. Res.*, **47**, 595–633.

Cox, M. D., 1970: A mathematical model of the Indian Ocean. *Deep-Sea Res.*, **17**, 47–75.

——, 1975: A baroclinic model of the World Ocean: Preliminary results. *Numerical Models of the Ocean Circulation*, National Academy of Sciences, Washington, D.C., 107–118.

——, 1976: Equatorially trapped waves and generation of the Somali Current. *Deep-Sea Res.*, **23**, 1139–1152.

——, 1980: Generation and propagation of 30-day waves in a numerical model of the Pacific. *J. Phys. Oceanogr.*, **10**, 1168–1186.

——, 1985: An eddy-resolving numerical model of the ventilated thermocline. *J. Phys. Oceanogr.*, **15**(10), 1312–1324.

——, 1987: An eddy-resolving numerical model of the ventilated thermocline: Time dependence. *J. Phys. Oceanogr.*, **17**(7), 1044–1056.

——, 1989: An idealized model of the World Ocean. Part I: The global scale water masses. *J. Phys. Oceanogr.*, **19**, 1730–1752.

——, and K. Bryan, 1984: A numerical model of the ventilated thermocline. *J. Phys. Oceanogr.*, **14**, 674–687.

Fiadeiro, M. E., 1982: Three-dimensional modeling of tracers in the deep Pacific Ocean II. Radiocarbon and the circulation. *J. Mar. Res.*, **40**, 537–550.

Holland, W. R., and A. D. Hirschman, 1972: A numerical calculation of the circulation in the North Atlantic Ocean. *J. Phys. Oceanogr.*, **2**, 336–352.

Ierley, G. R., and W. R. Young, 1983: Can the western boundary layer affect the potential vorticity distribution in the Sverdrup interior of a gyre? *J. Phys. Oceanogr.*, **13**, 1753–1763.

Legeckis, R., 1977: Long waves in the eastern equatorial Pacific. *Science*, **197**, 1179–1181.

Lighthill, M. J., 1969: Dynamic response of the Indian Ocean to the onset of the southwest monsoon. *Phil. Trans. Roy. Soc. London*, **A 265**, 45–92.

Luyten, J. R., J. Pedlosky and H. Stommel, 1983: The ventilated thermocline. *J. Phys. Oceanogr.*, **13**, 292–309.

Matsuno, T., 1966: Quasi-geostrophic motion in the equatorial region. *J. Meteor. Soc. Japan*, **44**, 25–43.

Munk, W., and E. Palmen, 1951: Note on the dynamics of Antarctic Circumpolar Current. *Tellus*, **3**, 53–56.

NAS, 1975: Numerical Models of Ocean Circulation. *Proc.*, Durham, NH, National Academy of Sciences,

Philander, S. G. H., 1978: Instabilities of zonal equatorial currents. Part II. *J. Geophys. Res.*, **83**, 3679–3682.

——, 1989: *El Niño, La Niña, and the Southern Oscillation.* Academic Press, 293 pp.

Phillips, N. A., 1956: The general circulation of the atmosphere: A numerical experiment. *Quart. J. Roy. Meteor. Soc.*, **82**, 123–164.

Piola, A. R., and A. L. Gordon, 1984: Pacific and Indian Ocean upper layer salinity budget. *J. Phys. Oceanogr.*, **14**, 747–753.

Rhines, P. B., and W. Young, 1982: A theory of wind-driven ocean circulation. I. Mid-ocean gyres. *J. Mar. Res.*, **40**(Suppl.), 559–596.

Sarkisyan, A. S., and V. F. Ivanov, 1971: The combined effect of baroclinicity and bottom topography as an important factor in the dynamics of ocean currents. *Izv. Acad. Sci. USSR Atmos. Ocean. Phys.*, **1**, 173–188.

Sarmiento, J. L., 1983: A simulation of bomb-tritium entry in the Atlantic Ocean. *J. Phys. Oceanogr.*, **13**, 1924–1939.

——, and K. Bryan, 1982: An ocean transport model for the North Atlantic. *J. Geophys. Res.*, **87**, 394–408.

——, C. G. Rooth and W. Roether, 1982: The North Atlantic tritium distribution in 1972. *J. Geophys. Res.*, **87**, 8047–8056.

Semtner, A. J., and R. M. Chervin, 1988: A simulation of the Global Ocean circulation with resolved eddies. *J. Geophys. Res.*, **93**, 15 502–15 522.

Schott, F., and H. Stommel, 1978: Beta spirals and absolute velocities in different oceans. *Deep-Sea Res.*, **25**, 961–1010.

Swallow, J. C., and J. G. Bruce, 1966: Current measurements off the Somali Coast during the southwest monsoon of 1964. *Deep-Sea Res.*, **13**, 861–888.

Toole, J. M., E. Zou and R. C. Millard, 1988: On the circulation of the upper waters in the western equatorial Pacific Ocean. *Deep-Sea Res.*, **35**, 1451–1482.

Whitworth, T., III, and R. G. Peterson, 1985: Volume transport of the Antarctic Circumpolar Current from bottom pressure measurements. *J. Phys. Oceanogr.*, **15**, 810–816.

Wunsch, C., 1978: The North Atlantic general circulation west of 50°W determined by inverse methods. *Rev. Geophys. Space Phys.*, **16**(4), 583–620.

——, D. Hu and B. Grant, 1983: Mass, heat, salt, and nutrient fluxes in the South Pacific Ocean. *J. Phys. Oceanogr.*, **13**, 725–753.

Wyrtki, K., and G. Meyers, 1976: The trade wind field over the Pacific Ocean. *J. Appl. Meteor.*, **15**, 698–704.